Article

Potential circadian effects on translational failure for neuroprotection

https://doi.org/10.1038/s41586-020-2348-z

Received: 16 August 2019

Accepted: 20 March 2020

Published online: 3 June 2020

Check for updates

Elga Esposito[1,5], Wenlu Li[1,5], Emiri T. Mandeville[1,5], Ji-Hyun Park[1,2], Ikbal Şencan[3], Shuzhen Guo[1], Jingfei Shi[1,4], Jing Lan[1,4], Janice Lee[1], Kazuhide Hayakawa[1], Sava Sakadžić[3], Xunming Ji[4] & Eng H. Lo[1]✉

Neuroprotectant strategies that have worked in rodent models of stroke have failed to provide protection in clinical trials. Here we show that the opposite circadian cycles in nocturnal rodents versus diurnal humans[1,2] may contribute to this failure in translation. We tested three independent neuroprotective approaches—normobaric hyperoxia, the free radical scavenger α-phenyl-butyl-tert-nitrone (αPBN), and the *N*-methyl-D-aspartic acid (NMDA) antagonist MK801—in mouse and rat models of focal cerebral ischaemia. All three treatments reduced infarction in day-time (inactive phase) rodent models of stroke, but not in night-time (active phase) rodent models of stroke, which match the phase (active, day-time) during which most strokes occur in clinical trials. Laser-speckle imaging showed that the penumbra of cerebral ischaemia was narrower in the active-phase mouse model than in the inactive-phase model. The smaller penumbra was associated with a lower density of terminal deoxynucleotidyl transferase dUTP nick end labelling (TUNEL)-positive dying cells and reduced infarct growth from 12 to 72 h. When we induced circadian-like cycles in primary mouse neurons, deprivation of oxygen and glucose triggered a smaller release of glutamate and reactive oxygen species, as well as lower activation of apoptotic and necroptotic mediators, in 'active-phase' than in 'inactive-phase' rodent neurons. αPBN and MK801 reduced neuronal death only in 'inactive-phase' neurons. These findings suggest that the influence of circadian rhythm on neuroprotection must be considered for translational studies in stroke and central nervous system diseases.

Circadian rhythms affect the mechanisms of disease and response to therapies[1,2]. Almost all experimental testing of neuroprotectants for stroke are performed during the day, when rodents are normally inactive. By contrast, clinical trials mostly recruit patients in whom strokes occurred during the day (when they are active) because of the need to establish time-of-onset. In five large clinical trials of neuroprotection in ischaemic stroke that involved 9,560 patients, only 664 had suffered night-time strokes (between 10.00 p.m. and 7.00 a.m.)[3]. We therefore investigated whether animal models mimic non-awake (inactive phase) strokes, whereas clinical trials test neuroprotection in awake (active phase) strokes (Fig. 1a).

We first assessed normobaric hyperoxia (NBO), a therapy that worked in rodents but did not succeed in clinical trials[4]. Male Sprague–Dawley rats were subjected to transient occlusion of the middle cerebral artery (MCAO) for 100 min and treated with 100% O_2 (NBO) or 30% O_2 (controls), and their brains were removed 24 h after onset of occlusion. NBO reduced infarction when experiments were performed during the day (inactive phase; zeitgeber time (ZT) 3–9) (Fig. 1b). However, NBO did not reduce infarction when experiments were performed at night (active phase; ZT15–21) (Fig. 1b). We noted that infarcts tended to be smaller when induced during the active phase. So, one possibility for the lack of neuroprotection might be because infarcts were already minimal and no further protection was possible. To control for this, we repeated these experiments with a less severe 60-min model of transient ischaemia. Untreated infarcts were now even smaller, but NBO was still able to reduce infarction at ZT3–9 (Fig. 1c).

A caveat with the NBO experiments was that the operator was not blinded to day versus night groups, and it is possible that operator performance decreased during night-time surgeries. To account for these issues, animals were housed in rooms with a normal or reversed light schedule for three weeks, and then all surgeries were performed during the day-time by operators blinded to light schedule. A different operator performed the surgeries, a different species was used, and a different neuroprotectant was tested. C57BL/6 male mice were subjected to transient MCAO for 60 min, then treated with the free radical scavenger αPBN[5] or vehicle immediately and 2 h after reperfusion. αPBN reduced infarct volumes (measured three days later) in mice operated on during the inactive (ZT3–9) but not the active phase (ZT15–21) (Fig. 1d).

To assess the generalizability of these results, we carried out a third series of experiments using a different model and neuroprotectant. C57BL/6 mice from rooms with a normal or reversed light schedule

[1]Neuroprotection Research Laboratories, Departments of Radiology and Neurology, Massachusetts General Hospital, Harvard Medical School, Boston, MA, USA. [2]College of Pharmacy, Seoul National University, Seoul, Korea. [3]Athinoula Martinos Center for Biomedical Imaging, Department of Radiology, Massachusetts General Hospital, Harvard Medical School, Boston, MA, USA. [4]Cerebrovascular Research Institute, XuanWu Hospital, Capital Medical University, Beijing, China. [5]These authors contributed equally: Elga Esposito, Wenlu Li, Emiri T. Mandeville. ✉e-mail: lo@helix.mgh.harvard.edu

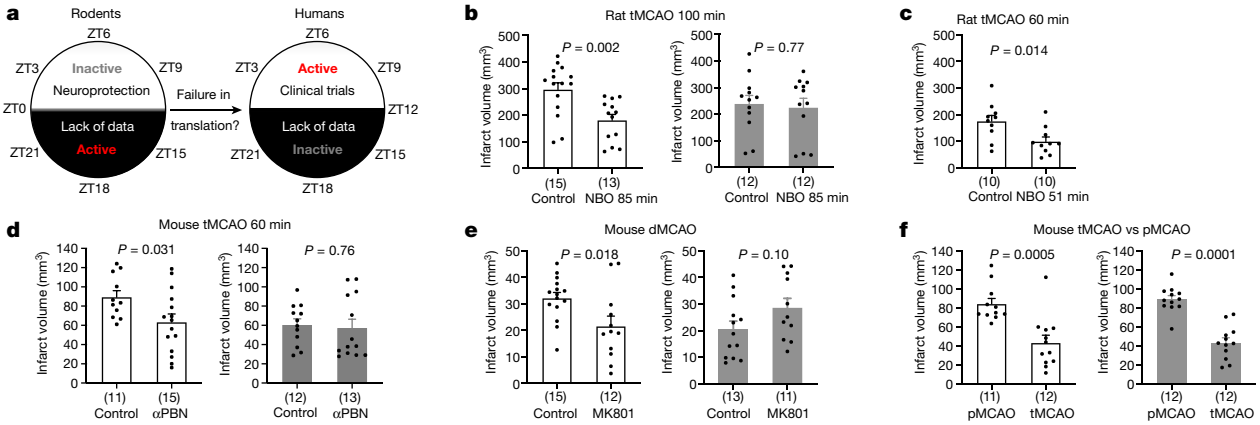

Fig. 1 | Neuroprotection in rodent models of stroke. a, Opposite circadian cycles in nocturnal rodents and diurnal humans. **b**, Transient MCAO (tMCAO) for 100 min in male Sprague–Dawley rats. Controls received 30% O_2. NBO group received 100% O_2 (for 85% of ischaemic period). NBO reduced infarction at ZT3–9 (left) but not ZT15–21 (right). **c**, NBO (for 85% of ischaemic period) reduced infarction after 60-min MCAO in Sprague–Dawley rats during ZT3–9. **d**, Treatment with αPBN (100 mg kg^{-1} intraperitoneally (IP) immediately and 2 h after reperfusion) reduced infarction after 60-min MCAO at ZT3–9 (left) but not ZT15–21 (right). **e**, MK801 (2.5 mg kg^{-1} IP, 1 h before occlusion) reduced infarction after permanent distal MCAO (dMCAO) at ZT3–9 (left) but not ZT15–21 (right). **f**, Infarct volumes were smaller in 60-min tMCAO versus permanent MCAO (pMCAO) in both ZT3–9 (left) and ZT15–21 (right) mice. All values mean ± s.e.m.; two-tailed *t*-test. For physiological parameters, laser-Doppler flow, and inclusion, exclusion and mortality information see Extended Data Table. 1. Infarct volumes quantified by triphenyltetrazolium (TTC) staining. Numbers in parentheses indicate animals per group.

were subjected to permanent ischaemia by coagulating and cutting the distal middle cerebral artery. Mice were treated with the NMDA receptor antagonist MK801[6] or vehicle 1 h before the onset of ischaemia. MK801 reduced 3-day infarct volumes in mice operated on during the inactive (ZT3–9) but not the active phase (ZT15–21) (Fig. 1e). The physiological parameters, including pH, p_{O_2}, p_{CO_2}, glucose and insulin levels, were similar across groups and fell within ranges consistent with models of cerebral ischaemia (Extended Data Table 1). In summary, three mechanistically independent, experimentally proven but clinically failed neuroprotectants all worked in ZT3–9 but not in ZT15–21 models. These results suggest that neuroprotection may be more difficult to achieve in active rodent models that are more similar to the patients (with day-time strokes) who are typically recruited to clinical stroke trials.

In contrast to the failures of neuroprotective strategies[7], the results of clinical trials have been positive for thrombolysis and thrombectomy[8,9], implying that reperfusion is a powerful treatment that works on both awake (active) and non-awake (inactive) strokes. C57BL/6 mice from rooms with a normal or reversed light schedule were subjected to MCAO, then randomized to undergo either permanent ischaemia or 60-min transient ischaemia. In this 'positive control' experiment, reperfusion decreased 24-h infarct volumes in mice operated on at either ZT3–9 or ZT15–21 (Fig. 1f). Circadian cycles may influence blood haemostasis pathways[10]. Therefore, we checked the clot lysis capacity of tissue plasminogen activator (tPA). There were no significant differences in tPA-clot lysis rates in mouse blood taken at ZT3–9 versus ZT15–21 (Extended Data Fig. 1).

Although our studies attempted to cover multiple models and targets, the importance of drug-specific and model-specific effects must be acknowledged. For example, we considered the possibility that by ameliorating reperfusion injury[11], αPBN could affect reperfusion blood flow differently in active and inactive mice. We subjected C57BL/6 mice to 60-min transient focal ischaemia, then treated them with αPBN or vehicle immediately and 2 h after reperfusion. Laser Doppler flowmetry showed no significant differences in reperfusion profiles across all groups (vehicle versus αPBN or ZT3–9 versus ZT15–21; Extended Data Fig. 2). For MK801, neuroprotection may be mediated by hypothermia[12]. To test whether MK801 affects temperature differently in active versus inactive mice, we treated C57BL/6 mice with MK801 or vehicle, then occluded the distal middle cerebral artery. There were no significant differences in rectal temperature across all groups (vehicle versus MK801 or ZT3–9 versus ZT15–21; Extended Data Fig. 3). Therefore, within the detection limits of our animal models, our observed circadian differences in αPBN and MK801 might not be confounded by large changes in reperfusion or temperature per se.

The penumbra is the conceptual target for neuroprotection in stroke[13,14]. It comprises areas in which blood flow is partially maintained, so neurons may transiently survive. Therefore, there may be two potential but not mutually exclusive reasons for our results—the penumbra is smaller and/or the penumbra responds differently to ischaemia and neuroprotection when animals are awake and active. To assess the first possibility, we subjected C57BL/6 mice from rooms with a normal or reversed light schedule to focal ischaemia, then performed laser-speckle imaging 25 min after occlusion. There were no significant differences in blood pressure and p_{CO_2} across all animals (Extended Data Fig. 4). As expected, there were blood flow gradients in the ipsilateral cortex, ranging from normal levels near the midline down to ischaemic levels in the core of the lesion (Fig. 2a). However, perfusion gradients were steeper in ZT17–19 than in ZT5–7 mice (Fig. 2a, b). The ischaemic penumbra (areas with intermediate perfusion: 30–50% of normal baseline[15,16]) was narrower in ZT17–19 than in ZT5–7 mice (Fig. 2b, c, Extended Data Fig. 5).

Without effective treatment, the penumbra collapses and the infarction grows. Therefore, another corollary of a smaller penumbra is that there should be less progressive cell death and reduced infarct growth after stroke onset. We subjected male C57BL/6 mice from rooms with a normal or reversed light schedule to 60-min transient focal ischaemia. As expected, infarct volumes grew between 12 and 72 h after occlusion, but the rate of infarct growth was reduced in ZT15–21 mice compared with ZT3–9 mice (Fig. 2d), consistent with a smaller penumbra. At 24 h post-ischaemia, the density of peri-infarct TUNEL-positive cells and the ratio of TUNEL to fluoro-jade-positive neurons were lower in ZT15–21 than in ZT3–9 penumbras (Fig. 2e, f). These results show that there is a smaller penumbra with less active cell death and reduced infarct growth in mouse stroke models in which the occlusion occurs during ZT15–21. These findings indirectly suggest that there may be less 'room to treat' in active rodent models that match patients with day-time stroke in neuroprotection trials.

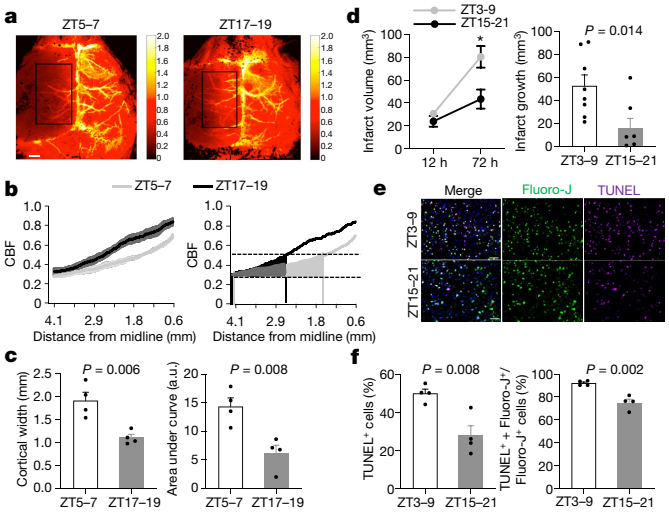

Fig. 2 | Comparisons of penumbra after focal cerebral ischaemia. a, Laser speckle imaging at 25 min post-MCAO at ZT5–7 and ZT17–19 in C57BL/6 mice. Rectangular area used for quantifying data from four independent experiments or mice per group in **b** and **c**. Scale bar, 1 mm. **b**, Ipsilateral blood flow gradients were steeper in ZT17–19 than in ZT5–7 images (left, line is mean, shaded areas are s.e.m.; right, area under the curve). **c**, The blood flow penumbra was operationally defined as average cortical width or area under the curve that was between 30 and 50% of normal levels, based on a lower threshold of infarction and an upper threshold of gene expression and protein synthesis inhibition (25–55 ml $100g^{-1}$ min^{-1}, see Methods and refs. [15,16]). The penumbra was narrower in mice operated on at ZT17–19 than at ZT5–7. Physiological parameters were similar across all animals (Extended Data Fig. 4). Penumbral perfusion was not correlated with blood pressure or p_{CO_2} ($r^2 = 0.006$ and 0.171, respectively). **d**, Infarct growth (12–72 h) after 60 min MCAO was smaller in mice operated on at ZT15–21 ($n = 8$) than at ZT3–9 ($n = 9$). **e**, Representative TUNEL, fluoro-jade and DAPI immunostaining in penumbral cortex at 24 h after 60 min MCAO in mice. Scale bar, 50 µm. **f**, Percentages of $TUNEL^+$ cells (out of DAPI cells) and of $TUNEL^+$ plus fluoro-$jade^+$ cells out of (fluoro-$jade^+$ cells) were lower in ZT15–21 penumbra than in ZT3–9 penumbra ($n = 4$ mice per group). Mean ± s.e.m.; two-tailed t-test.

Central circadian control resides in the suprachiasmatic nucleus, but circadian rhythms may also occur in the cortex[17,18]. We dissected somatosensory cortex from C57BL/6 mice and Sprague–Dawley rats, and measured expression of representative circadian genes using PCR with reverse transcription (RT–PCR). Our data confirmed that in this area, which is commonly affected in stroke, the temporal profile of circadian genes in mice and rats appears to be opposite to that found in human and nonhuman primate brains, consistent with the fact that rodents are nocturnal (Extended Data Fig. 6). We therefore investigated whether circadian cycles also directly affect neuronal susceptibility to ischaemia and response to neuroprotection.

We used dexamethasone to trigger circadian-like cycles of *Per1* and *Per2* expression in primary mouse cortical neurons[19] (Fig. 3a). These cycles allowed us to mimic in vivo experiments performed during the active phase (6 h post-dexamethasone, high *Per1* and *Per2*) or the inactive phase (12 h post-dexamethasone, low *Per1* and *Per2*). We deprived neurons of oxygen and glucose, treated cells with αPBN or MK801 during oxygen–glucose deprivation (OGD), re-oxygenated them for 24 h, and then performed cell viability assays to quantify neuroprotection (Fig. 3b). Deprivation of oxygen and glucose for 3 h led to 30–40% neuronal cell death. Although effect sizes were small, αPBN and MK801 appeared to significantly reduce cell death in 'inactive phase' but not 'active phase' rodent neurons (Fig. 3c, d).

As it was more difficult to protect 'active phase' than 'inactive phase' neurons, we looked for differences in targetable mechanisms in these neurons. After OGD, glutamate release and levels of reactive oxygen species (ROS) increased. However, these increases were smaller in 'active' than in 'inactive' neurons (Fig. 3e), suggesting that excitotoxicity and oxidative stress may be less prominent and therefore less therapeutically relevant in 'active' rodent neurons. Next, we looked at downstream cell death mechanisms, including apoptosis and necroptosis[20]. OGD induced activation of caspase-3 and RIP3 kinase, but these responses were also smaller in 'active' than in 'inactive' rodent neurons (Fig. 3f–h). After cerebral ischaemia, neurons die via both passive and active modes of cell death[21]. The former is a 'dissipative' cell death that occurs after severe loss of oxygen and glucose, which leads to metabolic collapse. These processes may occur in the core, and can be blocked only by prompt restoration of the missing energy substrates. The second is an 'active' mode that recruits upstream excitotoxicity and oxidative stress, and downstream apoptosis and necroptosis. This type of cell death is the conceptual target of molecular neuroprotection, presumably within the penumbra. Therefore, our in vitro results may be consistent with the in vivo finding that there is less active cell death and decreased infarct growth in ZT15–21 than in ZT3–9 stroke models, which implies that there should be less 'targetable injury' in ZT15–21 rodent models, which match patients who have had strokes during the day. A final proof-of-concept experiment was performed to examine this resistance to neuroprotection. Although it is impossible to block everything, we attempted to cover as many aspects of active cell death as possible: we used MK801 to block NMDA excitotoxicity, 2,3-dioxo-6-nitro-7-sulfamoyl-benzo[f]quinoxaline (NBQX) to block AMPA (α-amino-3-hydroxy-5-methyl-4-isoxazole propionic acid) excitotoxicity, αPBN to block ROS, zVAD-fmk to block apoptosis, and necrostatin-1 to block necroptosis, in neurons subjected to 3 h OGD and 24 h reoxygenation. Consistent with observed differences in active cell death, resistance to neuroprotection (that is, remaining injury after blocking these major active cell death targets) was greater in 'active' than 'inactive' rodent neurons (Fig. 3i).

Our findings point to a fundamental difference between currently used rodent models of neuroprotection and human patients with stroke. Clinical trials test neuroprotectants in active, awake patients, whereas rodent tests are performed during the day-time, when they are inactive. Nevertheless, there are caveats that must be kept in mind. First, circadian differences cannot be the only reason for translational failure. Other aspects of rodent models, including age, hypertension and metabolic disease, also do not match those of clinical populations. Indeed, the free radical spin trap NXY-059 was tested successfully in marmosets[22,23] (in two studies from a single laboratory) but still failed in clinical trials. Future studies are warranted to examine how circadian rhythms interact with age and comorbidities. Second, our study suggests that circadian rhythms affect the penumbra, but the underlying mechanisms of this effect remain unclear. How circadian rhythm affects neurovascular coupling in normal and ischaemic tissue should be explored[24,25]. Third, we showed a circadian influence on the neuronal response to OGD. Further studies are needed to dissect how neuroprotection is modulated by crosstalk between circadian genes and cell survival or death genes[26]. Fourth, our in vivo experiments focused on infarction. This approach will not work for drugs that promote recovery, so it is important to investigate how circadian cycles interact with neuroplasticity[27]. A fifth issue concerns stress. Although all groups were subjected to uniform handling methods and there were no detectable differences in cortisol (Extended Data Fig. 7), circadian differences may also involve unavoidable stress differences in active versus inactive rodents. Finally, circadian biology may interact with multiple aspects of stroke pathophysiology, including glial reactions, cytokines and chemokines, endothelial or haemostatic mechanisms, immune response, temperature regulation, the blood–brain barrier, and drug delivery or metabolism[28,29]. How these systems differ in active versus inactive rodent models must be investigated.

The failure of neuroprotection trials in patients with stroke have led to some pessimism in the field. However, recent successes with

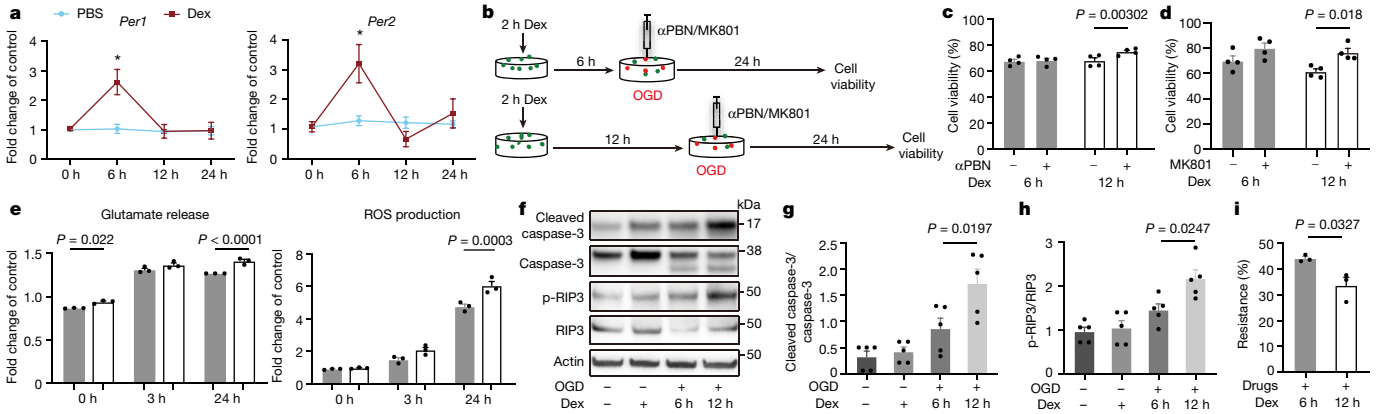

Fig. 3 | Effects of circadian cycles on response to OGD and neuroprotection. a, Primary mouse cortical neurons were treated for 2 h with dexamethasone (Dex). mRNA levels of *Per1* and *Per2* at 6 h and 12 h matched in vivo circadian cycles for rats and mice at ZT15–21 (upregulated *Per1* and *Per2*) and ZT3–9 (downregulated *Per1* and *Per2*), respectively. **P* = 0.0003 (*Per1*), **P* = 0.0026 (*Per2*), *n* = 3 independent experiments in triplicate. **b**, OGD in neurons treated with αPBN or MK801 after induction of circadian-like cycles in vitro. **c**, **d**, αPBN (**c**) and MK801 (**d**) were neuroprotective when *Per1* and *Per2* were downregulated (*n* = 4 independent experiments in triplicate). **e**, After 3 h OGD, glutamate release (left) and ROS production (right) were lower during times with upregulated *Per1* and *Per2* (*n* = 3 independent experiments in triplicate). **f**, Representative western blots of cleaved caspase-3, caspase-3, phosphorylated RIP3 kinase (p-RIP3) and RIP3 kinase at 24 h after OGD (gel source data in Supplementary Information; *n* = 5 independent experiments for densitometry). **g**, Quantification of cleaved caspase-3/caspase-3 ratio. **h**, Quantification of phosphorylated RIP3 kinase/RIP3 kinase ratio. **i**, 'Resistance to neuroprotection' after combination treatment with MK801 (10 μM), NBQX (50 μM), αPBN (1 μM), zVAD-fmk (50 μM) and necrostatin-1 (100 μM) (*n* = 3 independent experiments in triplicate). Mean ± s.e.m.; two-way ANOVA with Bonferroni adjustment (**a**, **c**–**e**), one-way ANOVA with post-hoc Tukey adjustment (**g**, **h**) or unpaired two-tailed *t*-test (**i**).

thrombectomy and reperfusion have led to calls to resume the quest[30]. Our findings suggest that, in order to move forward, stroke mechanisms and targets should be re-assessed in rodent models with the appropriate circadian context.

Online content

Any methods, additional references, Nature Research reporting summaries, source data, extended data, supplementary information, acknowledgements, peer review information; details of author contributions and competing interests; and statements of data and code availability are available at https://doi.org/10.1038/s41586-020-2348-z.

1. Logan, R. W. & McClung, C. A. Rhythms of life: circadian disruption and brain disorders across the lifespan. *Nat. Rev. Neurosci.* **20**, 49–65 (2019).
2. Cederroth, C. R. et al. Medicine in the fourth dimension. *Cell Metab.* **30**, 238–250 (2019).
3. VISTA Database http://www.virtualtrialsarchives.org/vista/ (2019).
4. Ding, J. et al. The effect of normobaric oxygen in patients with acute stroke: a systematic review and meta-analysis. *Neurol. Res.* **40**, 433–444 (2018).
5. Green, A. R., Ashwood, T., Odergren, T. & Jackson, D. M. Nitrones as neuroprotective agents in cerebral ischemia, with particular reference to NXY-059. *Pharmacol. Ther.* **100**, 195–214 (2003).
6. Schurr, A. Neuroprotection against ischemic/hypoxic brain damage: blockers of ionotropic glutamate receptor and voltage sensitive calcium channels. *Curr. Drug Targets* **5**, 603–618 (2004).
7. Neuhaus, A. A., Couch, Y., Hadley, G. & Buchan, A. M. Neuroprotection in stroke: the importance of collaboration and reproducibility. *Brain* **140**, 2079–2092 (2017).
8. Campbell, B. C., Meretoja, A., Donnan, G. A. & Davis, S. M. Twenty-year history of the evolution of stroke thrombolysis with intravenous alteplase to reduce long-term disability. *Stroke* **46**, 2341–2346 (2015).
9. Campbell, B. C. V. et al. Endovascular stent thrombectomy: the new standard of care for large vessel ischaemic stroke. *Lancet Neurol.* **14**, 846–854 (2015).
10. Pritchett, D. & Reddy, A. B. Circadian clocks in the hematologic system. *J. Biol. Rhythms* **30**, 374–388 (2015).
11. Schulz, J. B. et al. Facilitation of postischemic reperfusion with α-PBN: assessment using NMR and Doppler flow techniques. *Am. J. Physiol.* **272**, H1986–H1995 (1997).
12. Buchan, A. & Pulsinelli, W. A. Hypothermia but not the *N*-methyl-D-aspartate antagonist, MK-801, attenuates neuronal damage in gerbils subjected to transient global ischemia. *J. Neurosci.* **10**, 311–316 (1990).
13. Lo, E. H. A new penumbra: transitioning from injury into repair after stroke. *Nat. Med.* **14**, 497–500 (2008).
14. Donnan, G. A., Baron, J. C., Ma, H. & Davis, S. M. Penumbral selection of patients for trials of acute stroke therapy. *Lancet Neurol.* **8**, 261–269 (2009).
15. Heiss, W. D. Experimental evidence of ischemic thresholds and functional recovery. *Stroke* **23**, 1668–1672 (1992).
16. Hossmann, K. A. Viability thresholds and the penumbra of focal ischemia. *Ann. Neurol.* **36**, 557–565 (1994).
17. Mure, L. S. et al. Diurnal transcriptome atlas of a primate across major neural and peripheral tissues. *Science* **359**, eaao0318 (2018).
18. Chen, C. Y. et al. Effects of aging on circadian patterns of gene expression in the human prefrontal cortex. *Proc. Natl Acad. Sci. USA* **113**, 206–211 (2016).
19. Balsalobre, A. et al. Resetting of circadian time in peripheral tissues by glucocorticoid signaling. *Science* **289**, 2344–2347 (2000).
20. Fan, J., Dawson, T. M. & Dawson, V. L. Cell death mechanisms of neurodegeneration. *Adv. Neurobiol.* **15**, 403–425 (2017).
21. Lipton, P. Ischemic cell death in brain neurons. *Physiol. Rev.* **79**, 1431–1568 (1999).
22. Marshall, J. W., Duffin, K. J., Green, A. R. & Ridley, R. M. NXY-059, a free radical-trapping agent, substantially lessens the functional disability resulting from cerebral ischemia in a primate species. *Stroke* **32**, 190–198 (2001).
23. Marshall, J. W., Cummings, R. M., Bowes, L. J., Ridley, R. M. & Green, A. R. Functional and histological evidence for the protective effect of NXY-059 in a primate model of stroke when given 4 hours after occlusion. *Stroke* **34**, 2228–2233 (2003).
24. Paschos, G. K. & FitzGerald, G. A. Circadian clocks and vascular function. *Circ. Res.* **106**, 833–841 (2010).
25. Durgan, D. J., Crossland, R. F. & Bryan, R. M. Jr. The rat cerebral vasculature exhibits time-of-day-dependent oscillations in circadian clock genes and vascular function that are attenuated following obstructive sleep apnea. *J. Cereb. Blood Flow Metab.* **37**, 2806–2819 (2017).
26. Musiek, E. S. et al. Circadian clock proteins regulate neuronal redox homeostasis and neurodegeneration. *J. Clin. Invest.* **123**, 5389–5400 (2013).
27. Kobayashi, Y., Ye, Z. & Hensch, T. K. Clock genes control cortical critical period timing. *Neuron* **86**, 264–275 (2015).
28. Banks, W. A. From blood–brain barrier to blood–brain interface: new opportunities for CNS drug delivery. *Nat. Rev. Drug Discov.* **15**, 275–292 (2016).
29. Lo, E. H., Dalkara, T. & Moskowitz, M. A. Mechanisms, challenges and opportunities in stroke. *Nat. Rev. Neurosci.* **4**, 399–415 (2003).
30. Shi, L. et al. A new era for stroke therapy: integrating neurovascular protection with optimal reperfusion. *J. Cereb. Blood Flow Metab.* **38**, 2073–2091 (2018).

Methods

Animals

Male Sprague–Dawley rats (320–340 g) (Charles River Laboratories) were housed in a room with a standard light schedule: 12 h light (on) during the day (7.00 a.m.–7.00 p.m.) and 12 h dark (off) at night (7.00 p.m.–7.00 a.m.). Male C57BL/6 mice (25–28 g) (Charles River Laboratories) were randomly housed for 3 weeks before surgery and 1 or 3 days after surgery in two different rooms: with the standard light schedule the other with a switched cycle (12 h dark (off) during the day (7.00 a.m.–7.00 p.m.) and 12 h light (on) at night (7.00 p.m.–7.00 a.m.). Acclimatization and handling procedures were uniformly applied for all groups in all surgical, physiology, neuroprotection, gene expression and imaging experiments. However, it is noted that as part of the differences in circadian context, animals may unavoidably experience different levels of stress when experiments are performed during active or awake versus inactive or non-awake times. Experiments were approved by the Massachusetts General Hospital Institutional Animal Care and Use Committee (IACUC) in accordance with the National Institute of Health's Guide for the Care and Use of Laboratory Animals. All animals were randomly allocated to treatment groups.

Rat and mouse focal ischaemia

All animals were anaesthetized with isoflurane (1.5%) in 30%/70% oxygen/nitrous oxide. Transient focal ischaemia was induced by introducing a 6-0 (in mice) or 5-0 (in rats) surgical monofilament nylon suture (Doccol) from the external carotid artery into the internal carotid artery and advancing it to the branching point of the middle cerebral artery (MCA). Adequate ischaemia was confirmed by continuous laser Doppler flowmetry (LDF) (Perimed). Animals that did not have a significant reduction to less than 30% baseline LDF values during MCAO were excluded. After occluding the MCA for 60 min in mice and 100 min in rats, the monofilament suture was gently withdrawn in order to restore blood flow. In mice that underwent permanent proximal ischaemia the filament was left in the artery until the animal was euthanized. Rectal temperature was maintained at 37 °C with a thermostat-controlled heating pad.

Rats were randomized into control, 85′NBO groups or 61′NBO groups. The control group received 30% O_2 during all occlusion time. The 85′NBO group received 100% O_2 for 85 min, from 15 min after MCAO until the end of the occlusion. The 61′NBO group received 100% O_2 for 61 min, from 9 min after MCAO until the end of the occlusion. These timings are based on NBO protocols in the literature that have been shown to work in rodent models[31]. NBO was induced by exposing animals to 100% inspired oxygen. This is known to raise arterial p_{O_2} levels above 300 mm Hg.

Mice were divided into two groups: MCA occlusion control group and αPBN treatment group. αPBN (100 mg/kg, IP) was injected into mice immediately after reperfusion and 2 h later.

Distal permanent ischaemia in mice

Mice were anaesthetized with isoflurane under spontaneous respiration in a nitrous oxide/oxygen mixture. A burr hole (3 mm diameter) was drilled under saline cooling into the temporal bone overlying the distal MCA. The dura was kept intact. The exposed artery was occluded by microbipolar coagulation and cut between the lateral olfactory tract and the inferior cerebral vein.

The animals were divided into two groups: MCA occlusion control group and MK-801 treatment group. In the MK-801 treatment group, MK-801 (2.5 mg/kg) was administered intraperitoneally 1 h before MCA occlusion.

The exclusion criteria for transient and permanent focal ischaemia via intraluminal occlusions of the middle cerebral artery were based on laser Doppler flow (LDF; animals that did not have a significant reduction to less than 30% baseline during MCAO or in which LDF did not recover to 100% during reperfusion were excluded), surgery failure (that is, excessive bleeding during surgery) and animals euthanized for poor health conditions when suggested by veterinary staff. The exclusion criteria for permanent distal occlusion of the middle cerebral artery were based on surgery failure (that is, bleeding during surgery, artery occlusion in the wrong position or artery was not properly cut).

Cerebral ischaemia, treatments and circadian cycles

All experiments followed standard protocols for randomization of group assignment via four-number lottery draw, allocation concealment, blinding of operators, blinding of measurements and blinding of analyses. For a typical experiment, there should be four groups: day control, day drug, night control and night drug. Treatment dosing was based on extensive neuroprotection literature. NBO was administered as 100% inspired oxygen that results in arterial p_{O_2} above 300 mm Hg; this approach matches dosing in both experimental models and clinical trials[31]. Our doses of MK801 and αPBN were based on the extensive preclinical neuroprotection literature[32–35]. MK801 was tested in human trials of epilepsy and attention deficit disorders with repeated 0.15 mg/kg oral dosing[36]. The related spin trap NXY-059 was tested in patients with stroke using with intravenous infusions of 2,270 mg (5,940 μmol) per h, reduced after 1 h to 480–960 mg (1,260–2,520 μmol) per h for a further 71 h[37]. Our experiments were intended to test the idea that after cerebral ischaemia, response to these three potential neuroprotective therapies may be affected by circadian cycles. These studies do not unequivocally define all the ischaemia–circadian interaction mechanisms that may be involved[38–43].

Physiological parameters

Physiological parameters such as blood pressure, pH, p_{CO_2}, p_{O_2}, glucose and temperature were measured. Before surgery and αPBN treatment mean arterial pressure (mmHg) was measured in awake mice at ZT3–9 and ZT15–21. For αPBN treatment groups, the right femoral artery was cannulated with PE-10 polyethylene tubing and blood was collected 30 min after occlusion, 10 min after reperfusion and first drug injection and 24 h later (22 h after drug injection). For MK801 treatment groups, arterial blood was collected as well from the right femoral artery at 1 h after distal permanent occlusion (2 h after drug injection), and 24 h later (25 h after drug injection). In all groups, before collecting blood, at the same time points, blood pressure was measured. Body temperature was measured with a rectal temperature probe. Insulin and cortisol measurements were performed with the Ultra Sensitive Mouse Insulin ELISA Kit (Crystal Chem USA) and Cortisol ELISA Kit (Enzo), respectively, after blood was withdrawn from the posterior vena cava.

Laser speckle imaging

Mice were anaesthetized and focal ischaemia was induced using the filament method. To minimize breathing motion, the animal's head was restrained in a stereotaxic frame using ear bars. The scalp and the overlying membrane from the skull were gently incised down the midline and peeled to the side. Systemic arterial blood-gas measurement was performed at the end of each experiment to record p_{CO_2} and blood pressure (Extended Data Fig. 4). A laser diode (780 nm) was used for illumination and laser speckle images were recorded with a CMOS camera (acA1300-200μm, Basler), 25 min after occlusion. For each animal, three sets of raw speckle images were acquired in <15 s (300 frames in each set; image width, 1,280 pixels; image height, 1,024 pixels; pixel size, 11.72 μm; exposure time, 5 ms). A speckle contrast image was calculated from each raw speckle image using a sliding grid of 7 × 7 pixels. A mean speckle contrast image was calculated for each set and used to calculate the decorrelation time and relative cerebral blood flow (rCBF) at each pixel. The relative cerebral blood (rCBF) in the

ipsilateral (ischaemic) hemisphere was normalized by the mean rCBF in the contralateral (non-ischaemic) hemisphere. The mean lateral–medial profile of the rCBF was computed for the 4.1–0.6-mm range from the midline, within a coronal band between lambda and bregma. We defined the ischaemic penumbra as the cortical territory with rCBF values between 30 and 50% of baseline and estimated the width of the penumbra from the mean lateral–medial rCBF profile. These steps were repeated for each acquisition set. These thresholds were based on previously published operational definitions[15,16]. The ischaemic threshold for infarction (that is, the core) is approximately 20–25 ml/100 g/min. The threshold for gene expression and protein synthesis inhibition (that is, upper limit for penumbra) is approximately 50–60 ml/100 g/min. Based on rodent CBF values of approximately 110–120 ml/100 g/min, this corresponded to a penumbral range of 30–50%. Speckle imaging data were also expressed as absolute flow values by first confirming that mean speckle decorrelation times (t_c) were similar in healthy mice and in the nonischaemic hemisphere of mice with focal ischaemia ($1/t_c = 52.8 \pm 14.3$ and 61.2 ± 18.6 (mean ± s.d.), respectively), then recalculating all data based on 115 ml/100 g/min in mouse cortex. CBF data from all pooled hemispheres were plotted as histograms, and then thresholded to areas between 25 and 55 ml/100 g/min in individual mice for penumbral comparisons between day-time and night-time mice. All analysis was done using a custom script written in MATLAB (MathWorks). All analyses were randomized and operators were blinded.

Evaluation of infarct volume

The animals underwent transcardial perfusion with saline 1 or 3 days after ischaemia. Brains were quickly removed, placed within a brain matrix and cut into 7 (in rats) or 8 (in mice) coronal sections. The sections were then incubated in 2% TTC in saline for 10 min at room temperature. Infarction volumes were quantified using the 'indirect' morphometric method with Image J software. All analyses were carried out by operators blinded to conditions.

Primary neuron cultures and circadian gene induction

Primary neuron cultures were prepared from the cortex of embryonic day (E)17 C57BL/6 mouse embryos (Charles River Laboratory). In brief, the cortical tissues were dissected and digested with trypsin (Invitrogen). The cells were then plated onto poly-D-lysine-coated plates at a density of 3×10^5 cells/ml and cultured in DMEM (Life Technology, 11965-084) containing 5% fetal bovine serum (FBS). After 24 h, the medium was changed to NeuroBasal medium (Invitrogen, 21103-049) supplemented with 2% B-27 (Invitrogen, 17504044), 0.5 mM L-glutamine and 1% penicillin–streptomycin and replaced every 2–3 days. The neuron cells were cultured in humidified incubator at 37 °C and 5% CO_2 and were used for experiments from 8 to 11 days in vitro. To induce the circadian gene expression, neuron cultures were stabilized without changing the medium for 4 days, then dexamethasone (100 nM) was added and incubated for 2 h, after which the medium was replaced with regular NeuroBasal media. Cells were then harvested or subjected to OGD at indicated time points. These cell culture experiments only attempt to mimic circadian cycles, which are, by definition, a whole-organism in vivo phenomenon. However, these experiments may build on previous literature that have investigated the interactions between circadian genes and neuronal injury[26,43–45].

RT–PCR

Total mRNA was extracted using QIAzol lysis reagent (QIAGEN, 79306) and reverse transcribed using High-Capacity RNA-to-cDNA Kit (Thermo Fisher Scientific, 4387406) according to the manufacturer's instructions. The relative transcript level of circadian genes was measured using a Real Time PCR system (Applied Biosystems) using each primer for *Per1* (Applied Biosystems, Mm00501813), *Per2* (Mm00478099), and *Hprt1* (Mm01545399). Fold change in transcript level was calculated using $\Delta\Delta C_t$ normalized to 0 time samples.

OGD and reoxygenation

To induce OGD, the culture medium was replaced with deoxygenated, glucose-free DMEM (Life Technology, 11966-025) with or without neuroprotective reagents, MK-801 (10 μM) or αPBN (1 μM), and cells were placed in a humidified chamber (Heidolph, incubator 1000, Brinkmann Instruments) which was perfused with anaerobic gas mixture (90% N_2, 5% H_2, and 5% CO_2) for 30 min, then sealed and kept at 37 °C. After 2 h (αPBN) or 3 h (MK-801) of OGD, cultures were removed from the anaerobic chamber, and the medium was replaced with NeuroBasal medium supplemented with B-27 Minus AO (Invitrogen, 10889038) with or without the neuroprotective reagents. Cells were then allowed to recover for 24 h for a cell viability assay in a regular incubator.

Cell viability assays

Neuron cell injury was assessed by lactate dehydrogenase (LDH) assay using the Cytotoxicity Detection Kit (Roche Applied Science, 11644793001) according to the manufacturer's instructions. In brief, 500 μl of medium was collected and then centrifuged for 5 min at 500*g*. Fifty microlitres of supernatant was transferred to a 96-well plate in triplicate and 50 μl of dye/catalyst solution was added. The assay plates were then incubated at room temperature in the dark for 20 min and then the absorbance was read at 490 nm. For the MTT assay (Sigma, M2128), MTT reagent (final concentration 0.5 mg/ml) was added to neurons in 24-well plates and incubated at 37 °C for 3 h, then 200 μl of DMSO was added to solubilize the purple formazan. The absorbance was measured at 570 nm using a microplate reader. The relative assessments of neuronal injury were normalized by comparison with control cells as 100% cell survival.

Glutamate and ROS release assays

Glutamate production was measured using the Glutamate Assay Kit (Cell Biolabs, MET-5080). In brief, neuron cell culture supernatants were centrifuged at 10,000 rpm for 5 min to remove insoluble particles. Fifty microlitres of glutamate standard or each sample was added into the wells of a 96 well plate, and 200 μl of reaction mix or control mix was added to each well and mixed thoroughly. The mixture was incubated at room temperature for 60 min on an orbital shaker. The absorbance of each well was measured on a microplate reader using 450 nm as the primary wave length. ROS detection was measured by the carboxy derivative of fluorescein-carboxy-H2DCFDA (C400) which carries additional negative charges that improve its retention compared to noncarboxylated forms. In brief, neuron cell culture supernatants were removed. Cells were incubated in pre-warmed Hanks' balanced salt solution (HBSS) containing the probe to provide a final working concentration of 5 μM dye for 30 min. Then HBSS was removed and the cells were returned to pre-warmed medium and incubated at 37 °C for different times. The baseline fluorescence intensity of the loaded cells was determined before exposing the cells to experimental inducements. These glutamate and ROS measurements were intended as indirect in vitro markers to support the overall idea that there are stronger active cell death mechanisms in larger penumbras during active-phase strokes. A recent human study showed that higher plasma levels of oxidative stress biomarkers were indeed correlated with larger diffusion-perfusion MRI mismatch penumbras[46].

In vitro interaction of tPA and blood clots

Blood clots were prepared with 100 μl of heart ventricle blood. After 45 min of maturation at 37 °C with continuous shaking at 50 rpm, clots were moved from each Eppendorf tube into a 24-multiwell dish with 1.5 ml of saline solution for each well. Dissolution rates of blood clots were measured and the amount of haemoglobin released from the

clots over time was estimated. Clots were treated with 30 μg of tPA per clot. Clots were incubated at 37 °C with continuous shaking at 50 rpm for 180 min. At 0, 30, 90 and 180 min after treatment, 200 μl of supernatant was placed in a 96-multiwell dish, and the optical density (OD 415) of the haemoglobin released in the dissolution was measured in a microplate reader. The dissolution rate (DR) was measured with the following formula: $DR = (OD_{ti} - OD_{t0})/(t_i - t_0)$, where t_i and t_0 are two consecutive time points.

Immunohistochemistry

Samples were initially fixed with 4% paraformaldehyde for 10 min at room temperature. Then, samples were processed with 0.1% Triton X for 5 min, followed by 5% BSA blocking for 1 h at room temperature. The slides were then transferred to the TUNEL (Biotium, 30074) working solution for 1 h at 37 °C and then rinsed. To combine with fluoro-jade, the slides were then transferred to the fluoro-jade (Sigma, AG325) working solution for 10 min and then rinsed, air dehydrated and xylene cleared. Nuclei were counterstained with 4,6-diamidino-2-phenylindole (DAPI), and coverslips were placed. Immunostaining images were obtained using a fluorescence microscope (Nikon ECLIPSE Ti-S) or Nikon A1SiR Confocal Microscope.

Western blot analysis

Protein samples were loaded onto 4–12% Tris-glycine gels. After electorophoresis and transferring to nitro-cellulose membranes, the membranes were blocked in Tris-buffered saline containing 5% non-fat milk for 60 min at room temperature. Membranes were then incubated overnight at 4 °C with antibodies against caspase-3 (Cell Signaling Technology, 9662S), cleaved caspase-3 (Cell Signaling Technology, 9661S), RIP3 (Cell Signaling Technology, 95702), and phospho-RIP3 (Thr231/Ser232) (Cell Signaling Technology, 57220). After incubation with peroxidase-conjugated secondary antibodies, visualization was enhanced by chemiluminescence (GE Healthcare, NA931- anti-mouse, or NA934- anti-rabbit). Optical density was assessed using the NIH ImageJ analysis software.

Cell resistance

A cell counting kit (CCK)-8 (Dojindo) was used for determination of the number of viable cells. In brief, 20 μl reagent was added to mouse neuron cultures in 48-well plates at 37 °C for 1 h. The plates were then read using a standard plate reader with a reference wavelength of 450 nm. Background values from 630 nm were subtracted from those of 450 nm. The resistance of cells was measured with the following formula: $\text{resistance}\ (\%) = [1 - OGD_{drug}/Con_{drug}]/[1 - OGD_{dmso}/Con_{dmso}] \times 100$.

Statistical analysis

Results were expressed as mean ± s.e.m. All experiments were performed with randomization of group assignment via four-number lottery draw, allocation concealment, blinding of operators, blinding of measurements, and blinding of analyses. Sample size was predetermined using an online calculator: (https://www.danielsoper.com/statcalc/calculator.aspx?id=47) based on standard deviations and averages from historical and preliminary data ($\alpha = 0.05, 1 - \beta = 0.8$). When only two groups were compared, an unpaired two-tailed *t*-test was used. Multiple comparisons were evaluated by one-way or two-way ANOVA (with repeated measures when appropriate) followed by Tukey–Kramer tests or Bonferroni corrections. *P* values of less than 0.05 were considered statistically significant.

Reporting summary

Further information on research design is available in the Nature Research Reporting Summary linked to this paper.

Data availability

The datasets generated during and/or analysed during the current study are available from the corresponding author on reasonable request. Source Data associated with Figures and Extended Data are available online.

31. Poli, S. & Veltkamp, R. Oxygen therapy in acute ischemic stroke—experimental efficacy and molecular mechanisms. *Curr. Mol. Med.* **9**, 227–241 (2009).
32. Buchan, A. M., Slivka, A. & Xue, D. The effect of the NMDA receptor antagonist MK-801 on cerebral blood flow and infarct volume in experimental focal stroke. *Brain Res.* **574**, 171–177 (1992).
33. Cao, X. & Phillis, J. W. α-Phenyl-tert-butyl-nitrone reduces cortical infarct and edema in rats subjected to focal ischemia. *Brain Res.* **644**, 267–272 (1994).
34. Pschorn, U. & Carter, A. J. The influence of repeated doses, route and time of administration on the neuroprotective effects of BIII 277 CL in a rat model of focal cerebral ischemia. *J. Stroke Cerebrovasc. Dis.* **6**, 93–99 (1996).
35. Folbergrová, J., Zhao, Q., Katsura, K. & Siesjö, B. K. N-tert-butyl-alpha-phenylnitrone improves recovery of brain energy state in rats following transient focal ischemia. *Proc. Natl Acad. Sci. USA* **92**, 5057–5061 (1995).
36. Reimherr, F. W., Wood, D. R. & Wender, P. H. The use of MK-801, a novel sympathomimetic, in adults with attention deficit disorder, residual type. *Psychopharmacol. Bull.* **22**, 237–242 (1986).
37. Shuaib, A. et al. NXY-059 for the treatment of acute ischemic stroke. *N. Engl. J. Med.* **357**, 562–571 (2007).
38. Vinall, P. E., Kramer, M. S., Heinel, L. A. & Rosenwasser, R. H. Temporal changes in sensitivity of rats to cerebral ischemic insult. *J. Neurosurg.* **93**, 82–89 (2000).
39. Tischkau, S. A., Cohen, J. A., Stark, J. T., Gross, D. R. & Bottum, K. M. Time-of-day affects expression of hippocampal markers for ischemic damage induced by global ischemia. *Exp. Neurol.* **208**, 314–322 (2007).
40. Beker, M. C. et al. Time-of-day dependent neuronal injury after ischemic stroke: implication of circadian clock transcriptional factor Bmal1 and survival kinase Akt. *Mol. Neurobiol.* **55**, 2565–2576 (2018).
41. Ali, K., Cheek, E., Sills, S., Crome, P. & Roffe, C. Day-night differences in oxygen saturation and the frequency of desaturations in the first 24 hours in patients with acute stroke. *J. Stroke Cerebrovasc. Dis.* **16**, 239–244 (2007).
42. Kim, B. J. et al. Ischemic stroke during sleep: its association with worse early functional outcome. *Stroke* **42**, 1901–1906 (2011).
43. Karmarkar, S. W. & Tischkau, S. A. Influences of the circadian clock on neuronal susceptibility to excitotoxicity. *Front. Physiol.* **4**, 313 (2013).
44. Wang, T. A. et al. Circadian rhythm of redox state regulates excitability in suprachiasmatic nucleus neurons. *Science* **337**, 839–842 (2012).
45. Ghorbel, M. T., Coulson, J. M. & Murphy, D. Cross-talk between hypoxic and circadian pathways: cooperative roles for hypoxia-inducible factor 1α and CLOCK in transcriptional activation of the vasopressin gene. *Mol. Cell. Neurosci.* **22**, 396–404 (2003).
46. Lorenzano, S. et al. Early molecular oxidative stress biomarkers of ischemic penumbra in acute stroke. *Neurology* **93**, e1288–e1298 (2019).

Acknowledgements This study was supported in part by grants from the National Institutes of Health (K99MH120053 (I.Ş.), R01NS091230 and R01MH111359 (S.S.)), the Rappaport Foundation (E.H.L.), the Chinese Ministry of Education (X.J.), and the National Research Foundation of Korea (J.-H.P.). The authors thank J. Lipton, M. Ning and W. Deng for discussions, Y. Sun and all team members of the MGH 149-8 animal facility for help with light schedule switching, and M. Ali and K. R. Lees for generous assistance and expert analysis of the VISTA database.

Author contributions Performed experiments and/or analysed data: (E.E., W.L., E.T.M., J.-H.P., I. Ş., S.G., J.S., J. Lan, J. Lee, K.H.); designed experiments (E.E., W.L., E.T.M., J.-H.P., I. Ş., S.S., E.H.L.); wrote and/or revised manuscript (E.E., W.L., E.T.M., K.H., X.J., E.H.L.); funding and support (J.-H.P., S.S., X.J., E.H.L.).

Competing interests The authors declare no competing interests.

Additional information

Supplementary information is available for this paper at https://doi.org/10.1038/s41586-020-2348-z.

Correspondence and requests for materials should be addressed to E.H.L.

Peer review information *Nature* thanks John Hogenesch, Costantino Iadecola and the other, anonymous, reviewer(s) for their contribution to the peer review of this work.

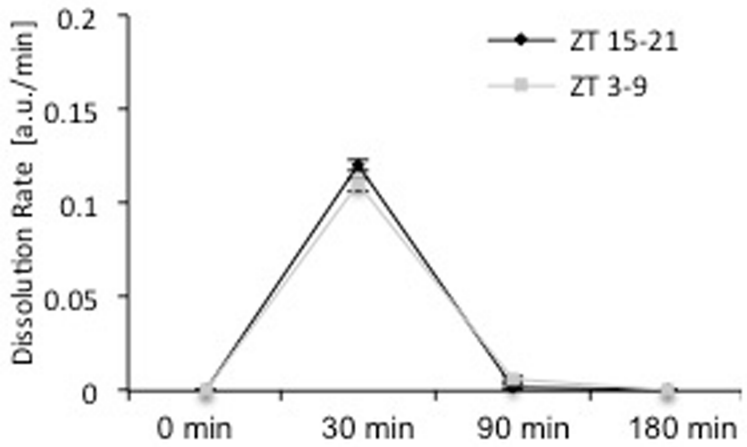

Extended Data Fig. 1 | Clot lysis. Rates of tissue-plasminogen activator-induced clot lysis were not significantly different in blood drawn from day-time (ZT3–9, $n = 5$) or night-time (ZT15–21, $n = 8$) male C57BL/6 mice. Mean ± s.e.m., repeated-measures ANOVA; $P = 0.80$.

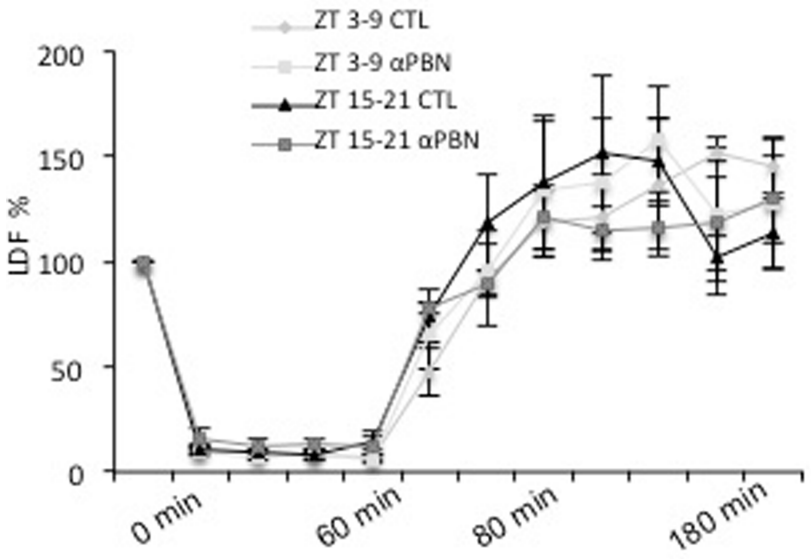

Extended Data Fig. 2 | Effects of αPBN on reperfusion. Laser Doppler flowmetry showed that αPBN (100 mg kg^{-1}) did not affect reperfusion profiles after 60-min transient focal ischaemia in ZT3–9 or ZT15–21 male C57BL/6 mice. Mean ± s.e.m., $n = 4$ per group, repeated-measures ANOVA; $P = 0.87$.

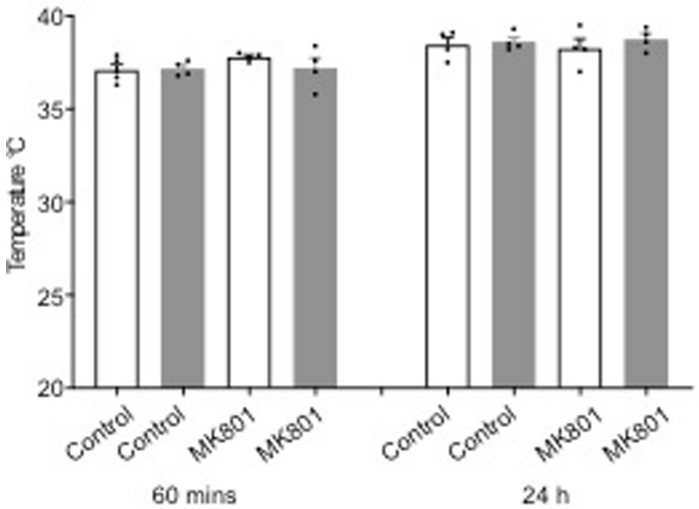

Extended Data Fig. 3 | MK801 did not significantly affect body temperature after permanent focal cerebral ischaemia. White bars, ZT3–9; grey bars, ZT15–21; male C57BL/6 mice. Mean ± s.e.m., $n = 4$ per group, repeated-measures ANOVA; $P = 0.97$.

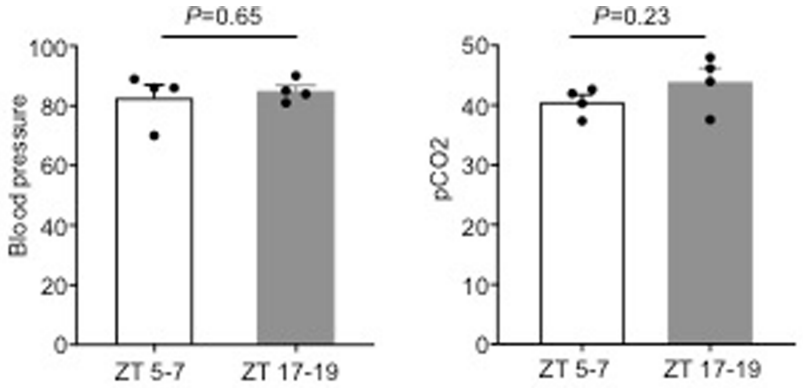

Extended Data Fig. 4 | Physiological parameters for laser speckle imaging experiments in Fig. 2. $n = 4$ mice per group; mean ± s.e.m., two-tailed t-test.

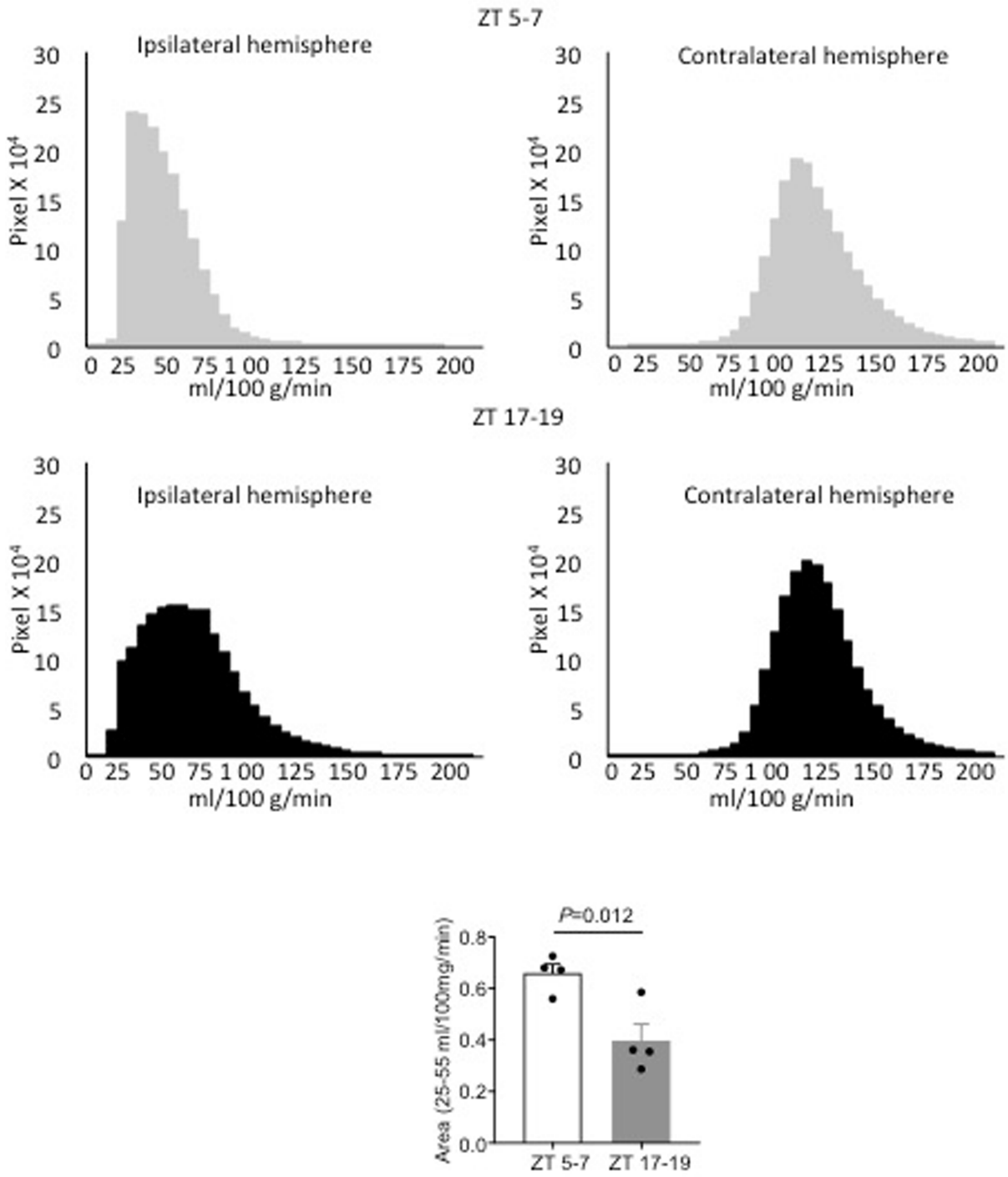

Extended Data Fig. 5 | Quantification of blood flow. Speckle imaging data were used to quantify blood flow in terms of absolute blood flow (ml per 100 g per min). Blood flow histograms show the presence of cerebral ischaemia in the ipsilateral hemispheres (top). Thresholded areas between 25 and 55 ml per 100 g per min (see Methods) were significantly smaller in ZT17–19 than in ZT5–7 C57BL/6 male mice (bottom; $n = 4$ per group, two-tailed t-test).

Expression of circadian genes in cortex of rodents and primates

ZT6	MOUSE	RAT	HUMAN/ PRIMATE	ZT18	MOUSE	RAT	HUMAN/ PRIMATE
Per1	⇩	⇩	⇧ *(cit. 17-18)*	Per1	⇧	⇧	⇩ *(cit. 17-18)*
Per2	⇩	⇩	⇧ *(cit. 17-18)*	Per2	⇧	⇧	⇩ *(cit. 17-18)*
Cry1	⇩	⇩	⇧ *(cit. 17)*	Cry1	⇧	⇧	⇩ *(cit.17.)*

Expression of circadian genes in cortex of rodents
(absolute levels relative to housekeeping gene Hprt1)

(n=6)	ZT 5-7		ZT 17-19	
Rat	Mean	SEM	Mean	SEM
Bmal1	0.292	0.008	0.323	0.005
Clock	0.645	0.027	0.796	0.026
Cry1	0.021	0.001	0.049	0.002
Cry2	1.564	0.148	2.117	0.167
Per1	0.735	0.168	1.416	0.146
Per2	0.036	0.004	0.123	0.005

(n=4)	ZT 5-7		ZT 17-19	
Mouse	Mean	SEM	Mean	SEM
Bmal1	0.275	0.020	0.297	0.019
Clock	0.493	0.036	0.512	0.037
Cry1	0.080	0.004	0.128	0.010
Cry2	0.337	0.018	0.354	0.026
Per1	0.562	0.100	0.855	0.063
Per2	0.086	0.009	0.175	0.015

Extended Data Fig. 6 | Circadian gene expression and patterns in different species. Top, comparison of circadian gene patterns between mice, rats, nonhuman primates and humans. Bottom, expression of selected circadian genes in C57BL/6 male mouse and Sprague–Dawley male rat somatosensory cortex ($n = 4$ per group).

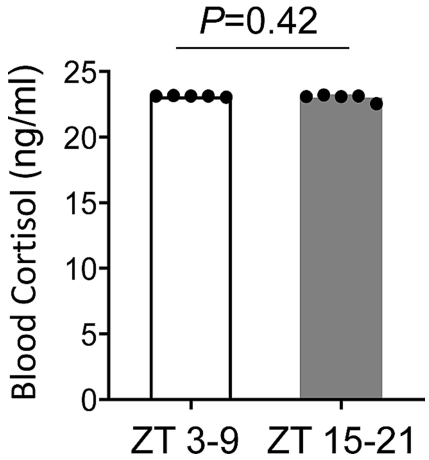

Extended Data Fig. 7 | Blood cortisol levels. No significant differences were detected in blood cortisol levels of ZT3–9 versus ZT15–21 C57BL/6 male mice subjected to similar handling procedures as cerebral ischaemia mice. Mean ± s.e.m., $n = 5$ mice per group, two-tailed t-test.

Extended Data Table 1 | Physiological parameters, laser doppler flow, mortality, inclusion and exclusions for neuroprotection experiments in Fig. 1

	ZT 3-9		ZT 15-21	
Mouse (n)	Control	PBN	Control	PBN
Total surgery	19	17	19	21
Total included	11	15	12	13
Excluded	3/19	0/17	4/19	6/21
Mortality	5/19	2/17	3/19	2/21

	ZT 3-9		ZT 15-21	
Mouse (n)	Control	MK801	Control	MK801
Total surgery	17	15	16	21
Total included	15	12	13	11
Excluded	2/17	3/15	3/16	9/21
Mortality	0/17	0/15	0/16	1/21

	ZT 3-9		ZT 15-21	
Rat (n)	Control	NBO 85'	Control	NBO 85'
Total surgery	24	21	15	16
Total included	15	13	12	12
Excluded	8/24	8/21	3/15	4/16
Mortality	1/24	0/21	0/15	0/16

	ZT 3-9		ZT 15-21	
Mouse (n)	Permanent	Transient	Permanent	Transient
Total surgery	18	13	15	16
Total included	11	12	12	12
Excluded	0/18	1/13	0/15	2/16
Mortality	7/18	0/13	3/15	2/16

	ZT 3-9	
Rat (n)	Control	NBO 51'
Total surgery	18	14
Total included	10	10
Excluded	8/18	4/14
Mortality	0/18	0/14

	ZT 3-9		ZT 15-21	
Mouse	Control	PBN	Control	PBN
0 min				
MAP [mmHg]	122±4.4	125±2.4	120±1.7	122±3.3
30 min				
MAP [mmHg]	94.6±5.39	88.3±3.29	87.6±3.40	86.5±3.45
pH	7.33±0.002	7.29±0.071	7.27±0.040	7.39±0.003
pO2 [mmHg]	182±23.4	154.75±12.3	177.5±11.9	185.8±15.4
pCO2 [mmHg]	40.2±1.80	40.5±3.63	46.6±5.32	35.4±1.14
Glu [mg/dL]	230.3±11.1	290±35.8	162.2±42.2	164.8±8.9
T [°C]	37.2±0.22	37.2±0.04	37.1±0.19	37.3±0.13
70 min				
MAP [mmHg]	89.5±2.39	82.3±2.57	85.7±2.25	79.5±2.5
pH	7.31±0.015	7.18±0.081	7.31±0.036	7.31±0.012
pO2 [mmHg]	189±23.9	155±15.6	149±26.7	183±15.24
pCO2 [mmHg]	43±0.97	44.8±4.59	43.7±3.85	38.5±1.17
Glu [mg/dL]	244.5±13.7	407.7±44.9	199.8±7.3	144.2±12.5
T [°C]	37.2±0.1	37.3±0.2	37.5±0.1	37.5±0.2
24 h				
MAP [mmHg]	79±6.33	78.7±5.15	77.5±6.81	76.6±3.11
pH	7.37±0.016	7.20±0.062	7.27±0.056	7.13±0.069
pO2 [mmHg]	232±17.4	199±25.6	229.2±7.7	185.7±16.4
pCO2 [mmHg]	34.7±1.4	38.1±3.1	38.1±1.5	46.1±3.2
Glu [mg/dL]	244.5±13.7	407.7±44.9	199.8±7.3	144.2±12.5
Insulin [ng/mL]	0.39±0.09	0.43±0.05	0.35±0.06	0.58±0.15
T [°C]	35.6±0.3	35.6±0.6	35.7±0.1	35.5±0.4

	ZT 3-9		ZT 15-21	
Mouse	Control	MK801	Control	MK801
60 min				
MAP [mmHg]	85±2.03	84.25±0.25	84.75±2.46	85.25±2.09
pH	7.35±0.019	7.29±0.019	7.4±0.01	7.33±0.004
pO2 [mmHg]	170±6.39	170±8.17	167.2±7.71	153±8.63
pCO2 [mmHg]	35.6±2.7	39.8±1.5	33.2±2.2	40.1±1
Glu [mg/dL]	327±21.3	343.7±18.3	282.5±27.2	272.8±29.8
Insulin [ng/mL]	0.83±0.12	1.05±0.32	0.64±0.12	0.98±0.28
24 h				
MAP [mmHg]	89.2±2.56	90.7±4.85	84.7±1.44	87.2±1.93
pH	7.41±0.008	7.36±0.01	7.39±0.029	7.37±0.003
pO2 [mmHg]	178.5±19.2	174.2±9.4	181.5±12.3	191.2±15.4
pCO2 [mmHg]	34.6±1.7	38.0±0.9	35.1±1.2	39.7±1.1
Glu [mg/dL]	211.7±10.4	240±30.1	181.2±13.3	199±22.1
Insulin [ng/mL]	0.53±0.12	0.38±0.07	0.84±0.51	0.82±0.26

	ZT 3-9		ZT 15-21	
Rat (60 min)	Control	NBO 85'	Control	NBO 85'
MAP [mmHg]	101±5.1	108±2.7	98.2±5.7	102.7±10.7
pH	7.45±0.018	7.38±0.003	7.41±0.030	7.40±0.016
pO2 [mmHg]	180±7.4	462.2±11.33	206.2±11.12	468.7±20.03
pCO2 [mmHg]	37.4±2.62	45.5±2.08	41.6±3.03	45.5±3.72
LDF(%)	26±1.64	26.6±1.67	26.2±1.58	26.6±2.45

nature research

Corresponding author(s): Eng H. Lo

Last updated by author(s): Mar 16, 2020

Reporting Summary

Nature Research wishes to improve the reproducibility of the work that we publish. This form provides structure for consistency and transparency in reporting. For further information on Nature Research policies, see Authors & Referees and the Editorial Policy Checklist.

Statistics

For all statistical analyses, confirm that the following items are present in the figure legend, table legend, main text, or Methods section.

n/a	Confirmed	
☐	☒	The exact sample size (*n*) for each experimental group/condition, given as a discrete number and unit of measurement
☐	☒	A statement on whether measurements were taken from distinct samples or whether the same sample was measured repeatedly
☐	☒	The statistical test(s) used AND whether they are one- or two-sided *Only common tests should be described solely by name; describe more complex techniques in the Methods section.*
☐	☒	A description of all covariates tested
☐	☒	A description of any assumptions or corrections, such as tests of normality and adjustment for multiple comparisons
☐	☒	A full description of the statistical parameters including central tendency (e.g. means) or other basic estimates (e.g. regression coefficient) AND variation (e.g. standard deviation) or associated estimates of uncertainty (e.g. confidence intervals)
☐	☒	For null hypothesis testing, the test statistic (e.g. *F*, *t*, *r*) with confidence intervals, effect sizes, degrees of freedom and *P* value noted *Give P values as exact values whenever suitable.*
☒	☐	For Bayesian analysis, information on the choice of priors and Markov chain Monte Carlo settings
☒	☐	For hierarchical and complex designs, identification of the appropriate level for tests and full reporting of outcomes
☐	☒	Estimates of effect sizes (e.g. Cohen's *d*, Pearson's *r*), indicating how they were calculated

Our web collection on statistics for biologists contains articles on many of the points above.

Software and code

Policy information about availability of computer code

Data collection	No softwares were used to collect data.
Data analysis	Infarction volumes were quantified on TTC stained sections using the “indirect” morphometric method (Lin et al., 1993) with Image J. Statistical analysis were performed with GraphPad Prism 6.01. For Speckle Imaging all analysis was done by using a custom script written in MATLAB (MathWorks).

For manuscripts utilizing custom algorithms or software that are central to the research but not yet described in published literature, software must be made available to editors/reviewers. We strongly encourage code deposition in a community repository (e.g. GitHub). See the Nature Research guidelines for submitting code & software for further information.

Data

Policy information about availability of data

All manuscripts must include a data availability statement. This statement should provide the following information, where applicable:

- Accession codes, unique identifiers, or web links for publicly available datasets
- A list of figures that have associated raw data
- A description of any restrictions on data availability

The authors declare that the data supporting the findings of this study are available within the paper and its supplementary information files or from the corresponding author upon reasonable request.

Field-specific reporting

Please select the one below that is the best fit for your research. If you are not sure, read the appropriate sections before making your selection.

☒ Life sciences ☐ Behavioural & social sciences ☐ Ecological, evolutionary & environmental sciences

For a reference copy of the document with all sections, see nature.com/documents/nr-reporting-summary-flat.pdf

Life sciences study design

All studies must disclose on these points even when the disclosure is negative.

Sample size	Sample size was predetermined using the software available online: https://www.danielsoper.com/statcalc/calculator.aspx?id=47 The calculation was based on Cohen's d value where SD and average were estimated from our historical and preliminary data.
Data exclusions	The exclusion criteria for transient and permanent focal ischemia via intraluminal occlusions of the middle cerebral artery were based on LDF (animals that did not have a significant reduction to less than 30% baseline during MCAO or LDF was not recovered to 100% during reperfusion were excluded), surgery failure (i.e. excessive bleeding during surgery) and animals euthanized for poor health conditions when suggested by veterinary. The exclusion criteria for permanent distal occlusion of the middle cerebral artery were based on surgery failure (i.e. bleeding during surgery, artery occlusion in the wrong position or artery was not properly cut).
Replication	For in vitro experiments, each experiment was repeated at least 3 times. Details are in the method section
Randomization	All experiments followed standard protocols for randomization of group assignment via 4 number lottery draw, allocation concealment, blinding of operators, blinding of measurements, blinding of analyses. For a typical experiment, there should be 4 groups: day control, day drug, night control, night drug.
Blinding	All procedures and measurements were performed in a blinded and randomized fashion.

Reporting for specific materials, systems and methods

We require information from authors about some types of materials, experimental systems and methods used in many studies. Here, indicate whether each material, system or method listed is relevant to your study. If you are not sure if a list item applies to your research, read the appropriate section before selecting a response.

Materials & experimental systems

n/a	Involved in the study
☒	☐ Antibodies
☒	☐ Eukaryotic cell lines
☒	☐ Palaeontology
☐	☒ Animals and other organisms
☒	☐ Human research participants
☒	☐ Clinical data

Methods

n/a	Involved in the study
☒	☐ ChIP-seq
☒	☐ Flow cytometry
☒	☐ MRI-based neuroimaging

Animals and other organisms

Policy information about studies involving animals; ARRIVE guidelines recommended for reporting animal research

Laboratory animals	Male Sprague-Dawley rats (320 to 340 g) and male C57BL/6 male mice (23 to 27 g) were used in this study.
Wild animals	No wild animals were used in this study.
Field-collected samples	No field-collected were used in this study.
Ethics oversight	All experiments were performed following an institutionally approved protocol in accordance with National Institutes of Health guidelines and with the United States Public Health Service's Policy on Human Care and Use of Laboratory Animals and following Animals in Research: Reporting In vivo Experiments (ARRIVE) guidelines.

Note that full information on the approval of the study protocol must also be provided in the manuscript.